GEOPHYSICS, VOL. 49, NO. 4 (APRIL 1984); P. 453–466, 11 FIGS., 2 TABLES.

Heat flow in the Uinta Basin determined from bottom hole temperature (BHT) data

David S. Chapman*, T. H. Keho*, Michael S. Bauer*, and M. Dane Picard*

ABSTRACT

The thermal resistance (or Bullard) method is used to judge the utility of petroleum well bottom-hole temperature data in determining surface heat flow and subsurface temperature patterns in a sedimentary basin. Thermal resistance, defined as the quotient of a depth parameter Δz and thermal conductivity k, governs subsurface temperatures as follows:

$$T_B = T_0 + q_0 \sum_{z=0}^{B} \left(\frac{\Delta z}{k}\right),$$

where T_B is the temperature at depth $z = B$, T_0 is the surface temperature, q_0 is surface heat flow, and the thermal resistance ($\Delta z/k$) is summed for all rock units between the surface and depth B. In practice, bottom-hole and surface temperatures are combined with a measured or estimated thermal conductivity profile to determine the surface heat flow q_0 which, in turn, is used for all consequent subsurface temperature computations.

The method has been applied to the Tertiary Uinta Basin, northeastern Utah, a basin of intermediate geologic complexity—simple structure but complex facies relationships—where considerable well data are available. Bottom-hole temperatures were obtained for 97 selected wells where multiple well logs permitted correction of temperatures for drilling effects. Thermal conductivity values, determined for 852 samples from 5 representative wells varying in depth from 670 to 5180 m, together with available geologic data were used to produce conductivity maps for each formation. These maps show intraformational variations across the basin that are associated with lateral facies changes. Formation thicknesses needed for the thermal resistance summation were obtained by utilizing approximately 2000 wells in the WEXPRO Petroleum Information file. Computations were facilitated by describing all formation contacts as fourth-order polynomial surfaces.

Average geothermal gradient and heat flow for the Uinta Basin are 25°C km^{-1} and 57 mW/m^2, respectively. Heat flow appears to decrease systematically from 65 to 40 mWm^{-2} from the Duchesne River northward toward the south flank of the Uinta Mountains. This decrease may be the result of refraction of heat into the highly conductive quartzose Precambrian Uinta Mountain Group. More likely, however, it is related to groundwater recharge in late Paleozoic and Mesozoic sandstone and limestone beds that flank the south side of the Uintas. Heat flow values determined for the southeast portion of the basin show some scatter about a mean value of 64 mWm^{-2} but no systematic variation.

INTRODUCTION

Bottom-hole temperatures (BHT) obtained from routine geophysical logs of petroleum wells comprise, for good reasons, a little used data set in geothermal and heat flow studies. The bottom-hole temperature (and consequently the thermal gradient), and the thermal conductivity profile, both required for heat flow determinations and reasonable interpretation of temperature data, are unobtainable with confidence from routine geophysical logs of the wells taken soon after the completion of drilling. Even if accurate temperature measurements are made (which generally is unnecessary in petroleum well logging), temperatures in and around wells are perturbed by the drilling process, principally by the circulation of mud at a temperature that differs from in-situ conditions. There is seldom sufficient information to make accurate corrections for the perturbation.

Manuscript received by the Editor March, 1983; revised manuscript received September, 1983.
*Department of Geology and Geophysics, University of Utah, 717 W. C. Browning Bldg., Salt Lake City, UT 84112-1183.

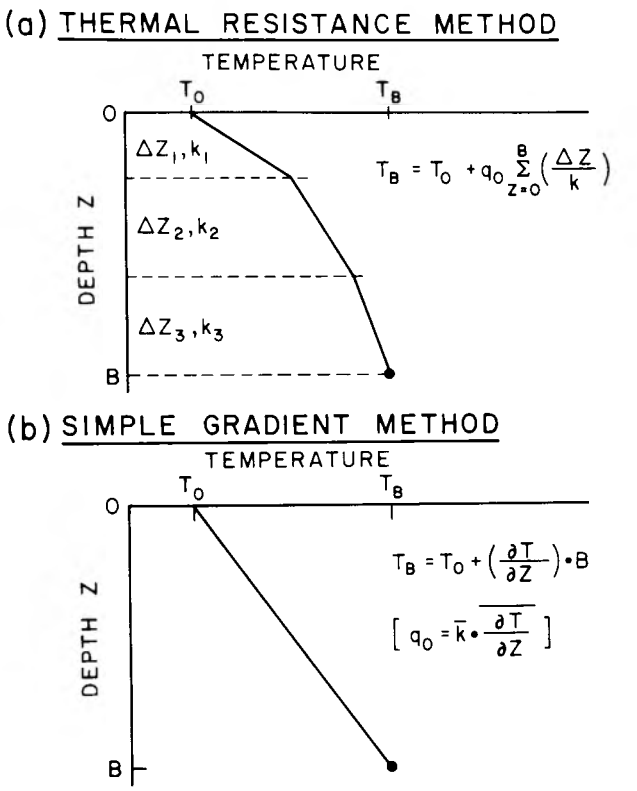

FIG. 1. Schematic representation of two methods for processing BHT data from oil and gas wells: (a) thermal resistance method and (b) simple gradient method. Symbols: T_0 surface temperature, T_B bottom-hole temperature, q_0 surface heat flow, z depth, k thermal conductivity.

Assigning thermal conductivity values for any particular drill hole is more problematic. Thermal conductivities are not routinely measured and general predictive relationships between conductivity and parameters determined in routine geophysical logs are not always reliable (Goss, 1974; Vacquier, 1981). Thus, spatial variations in thermal gradients deduced from BHTs may be either spurious because of errors in the temperature data or, in the case of the gradients being fortuitously correct, the ambiguity in interpreting gradient patterns in terms of tectonic or hydrologic processes rather than conductivity variations will be unresolved.

Despite these difficulties, it is possible, especially upon application of temperature corrections and conductivity measurements, to obtain useful information from BHT data in individual cases. Pertinent studies are Evans and Tammemagi (1974) on the Somalian Horn and Sudan; Evans and Coleman (1974) on North Sea oil fields; Carvalho and Vacquier (1977) on the Reconcavo Basin of Brazil; Carvalho et al (1980) on central Sumatra; Hodge et al (1980) on upper New York State; and Reiter and Tovar (1982) on northern Chihuahua, Mexico. Unfortunately, the most comprehensive study of bottom-hole temperatures in the coterminous USA (AAPG Geothermal Survey of North America, 1976) ignores thermal conductivity effects which makes their thermal gradient maps of limited use.

In this paper we use the thermal resistance method pioneered by Bullard (1939) to determine and evaluate lateral heat flow variations within a single basin and to produce subsurface temperature maps within the basin. Our method does not totally alleviate problems that arise from nonequilibrium temperature logs and incomplete description of thermal conductivity patterns, but it does have as a basis corrected temperature data and measured thermal conductivity values. Further, we do not restrict individual oil and gas fields to a homogenized single gradient and single conductivity function as was done by Carvalho and Vacquier (1977), but instead we allow for lateral changes in several parameters including surface temperature, thermal conductivity, and heat flow. The effects of porosity and temperature on the formation thermal conductivity and hence thermal resistance are also included. The Tertiary Uinta Basin of northeastern Utah is chosen to illustrate our thermal resistance method because of its intermediate geologic complexity, i.e., simple structure but complex facies patterns, and the abundance of petroleum well data.

Thermal resistance method

Thermal resistance is the quotient of a thickness Δz and a characteristic thermal conductivity k. In the case of negligible heat production and fluid movement, subsurface temperatures in horizontally layered, isotropic earth are governed by the thermal resistance of a stratigraphic section in the following way (Bullard, 1939; and Figure 1a):

$$T_B = T_0 + q_0 \sum_{z=0}^{B} \left(\frac{\Delta z}{k}\right), \tag{1}$$

where T_B is the temperature at depth $z = B$, T_0 is the surface temperature at $z = 0$, q_0 is surface heat flow, and the thermal resistance $(\Delta z/k)$ is summed for all rock units between the surface and depth B. This equation, or the integral form of it, is commonly used in heat flow data reduction, and heat flow (q_0) is calculated as the slope of the plot of consecutive values of T_B versus the summed thermal resistance to the measurement depth. The method is especially suitable when boreholes intersect discrete and horizontal rock units.

The thermal resistance method, as we use it for analysis of heat flow and subsurface temperatures in a sedimentary basin, comprises several steps. First, a set of bottom-hole temperatures (T_B) are compiled and corrected, if possible, for drilling disturbances. The wells from which temperatures are taken should represent a wide geographic distribution throughout the basin. This is not always possible, however, since wells are drilled preferentially in favored localities. Second, thermal conductivity values must be measured for all representative rocks in the basin: drill chips, core samples, and outcrop samples can be used. Laboratory results for conductivities must be modified for effects of temperature, porosity, and possibly anisotropy to simulate in-situ conditions. Temperature-depth profiles and thermal conductivity-depth profiles are allowed to vary with lateral position in the basin. The third step involves summing the thermal resistance at each well from the surface to the depth of the BHT observation and solving for the site heat flow using equation (1).

Ideally, the thermal resistance sum is calculated individually for each well using conductivities and thicknesses for all rock units intersected (Carvalho et al, 1980). This individual well treatment is cumbersome, however, for large numbers of wells. An automatic processing procedure is useful if the basin structure is sufficiently simple and well known so that contacts

between rock units and conductivity variations are describable by simple functions. In the Uinta Basin, formation contact depths are adequately described in terms of low-order polynomial surfaces. The modified form of equation (1) used to calculate individual site heat flow values is

$$q_0(x, y) = [T_{B,\infty}(x, y) - T_0(x, y, h)] \Big/ \sum_{z=0}^{B} \frac{\Delta z(x, y)}{k(x, y, z, \phi, T)}, \tag{2}$$

ϕ being the depth and lithology dependent porosity. For each well the latitude and longitude (equivalently x and y), well collar elevation h, corrected bottom-hole temperature $T_{B,\infty}$, and corresponding depth $z = B$ are stored in a data file. Surface temperature as a function of position, and elevation $T_0(x, y, h)$, rock unit thickness $\Delta z(x, y)$ as a function of position, and thermal conductivity $k(x, y, z, \phi, T)$ as a function of position and depth are calculated from empirical functions. Once surface heat flow values are determined from equation (2) for the wells sampled, and the heat flow field is suitably smoothed, subsurface temperature maps can be calculated by a direct application of the thermal resistance method. Principal features of this procedure as applied to the Unita Basin are given in Table 1; details are discussed later in the text.

The simple gradient method (Klemme, 1975; Chaturvedi and Lory, 1980; Lam et al, 1982) is an alternative approach to analyzing BHT data. Thermal gradients are calculated either as two-point differences using a single BHT and an estimate of the mean annual ground temperature or through regression techniques on multiple bottom-hole temperatures at different depths. This technique for treating BHT data is shown schematically in Figure 1b. The single advantage of the simple gradient method is its convenience: BHT information is commonly stored and available in data files. Scatter in uncorrected temperatures for a common depth in any petroleum field, however, is typically 10° to 20°C (Carvalho and Vacquier, 1977, Figures 3–8) which leads to large uncertainties in the computed gradient. Correction of data for drilling effects reduces scatter but is often not possible from information stored in data files. Also, without thermal conductivity information, the explanation of the scatter is unclear. Our thermal resistance method requires the measurement or estimation of thermal conductivity values but, in return, provides an estimate of actual temperature errors and of lateral heat flow variations.

We now present our application of the thermal resistance method to the problem of heat flow and subsurface temperature variations within the Uinta Basin. The geologic setting of the basin and the basic information available from petroleum exploration are described first. Analyses of temperature and thermal conductivity data and corrections which may be applied to them are then discussed separately. Finally, the heat flow and subsurface temperature maps are presented.

Table 1. Application of thermal resistance method to Uinta Basin study.

Equation (2): $q_0(x, y) = [T_{B,\infty}(x, y) - T_0(x, y, h)] \Big/ \sum_{z=0}^{B} \frac{\Delta z(x, y)}{k(x, y, z, \phi, T)}$

Symbol	Parameter	Procedure/corrections
$T_{B,\infty}$	Bottom-hole temperature at equilibrium (i.e., infinite elapsed time)	Correct for drilling disturbance $T_B(t_e) = T_{B,\infty} + A \log\left(\frac{t_c + t_e}{t_e}\right)$
$T_0(x, y, h)$	Surface ground temperature	Correct for elevation and air lapse rate $T_0(x, y, h) = 22.4 - 0.0067h$ where h is elevation in meters, T_0 in °C
$\Delta z(x, y)$	Unit thickness	Describe formation thicknesses in terms of differences between fourth-order polynominal surfaces $\Delta z_{Fm} = z_j(x, y) - z_i(x, y)$ where z_i, z_j are depths to tops of formations i and j, respectively; z_j may be depth to measurement point.
$k(x, y, z, \phi, T)$	Thermal conductivity	Correct lab measurement of solid component k_s at room temperature to in-situ conditions of variable porosity and temperature $k_r = k_w^{\phi} k_s^{(1-\phi)}$
ϕ	Porosity	$\phi = 0.25 \exp(-z/3.0)$ where z is depth in kilometers
k_w	Thermal conductivity of water	$k_w = 0.56 + 0.003T^{0.827}$; $0 \le T \le 63$°C $k_w = 0.481 + 0.942 \ln T$; $T > 63$°C
k_s	Thermal conductivity of solid matrix	$k_s = k_{s,20}\left(\frac{293}{273 + T}\right)$ where $k_{s,20}$ is laboratory result and T is formation temperature in °C

Geologic setting of Uinta Basin

The Unita Basin is an intraplate sedimentary basin within the northern Colorado Plateau (Figure 2). The geographic basin is bounded on the south by the Book Cliffs, on the west by the southern and central Wasatch Mountains, on the north by the Uinta Mountains, and on the east by the Douglas Creek arch. The basin is roughly elliptical, stretching 210 km along its major east-west axis and 160 km in a north-south direction. It occupies an area of approximately 20,000 km^2 (Picard and High, 1972).

The pre-Tertiary stratigraphic history of the Uinta Basin is one of regularity and stability (Preston, 1957; Untermann and Untermann, 1964). Rock formations range in age from Precambrian through Tertiary, but Mississippian beds uncomformably overlie Cambrian beds. Periods of marine and continental deposition occurred with nonmarine deposition dominant after the Permian (Bruhn et al, 1983). Total thickness of beds ranges

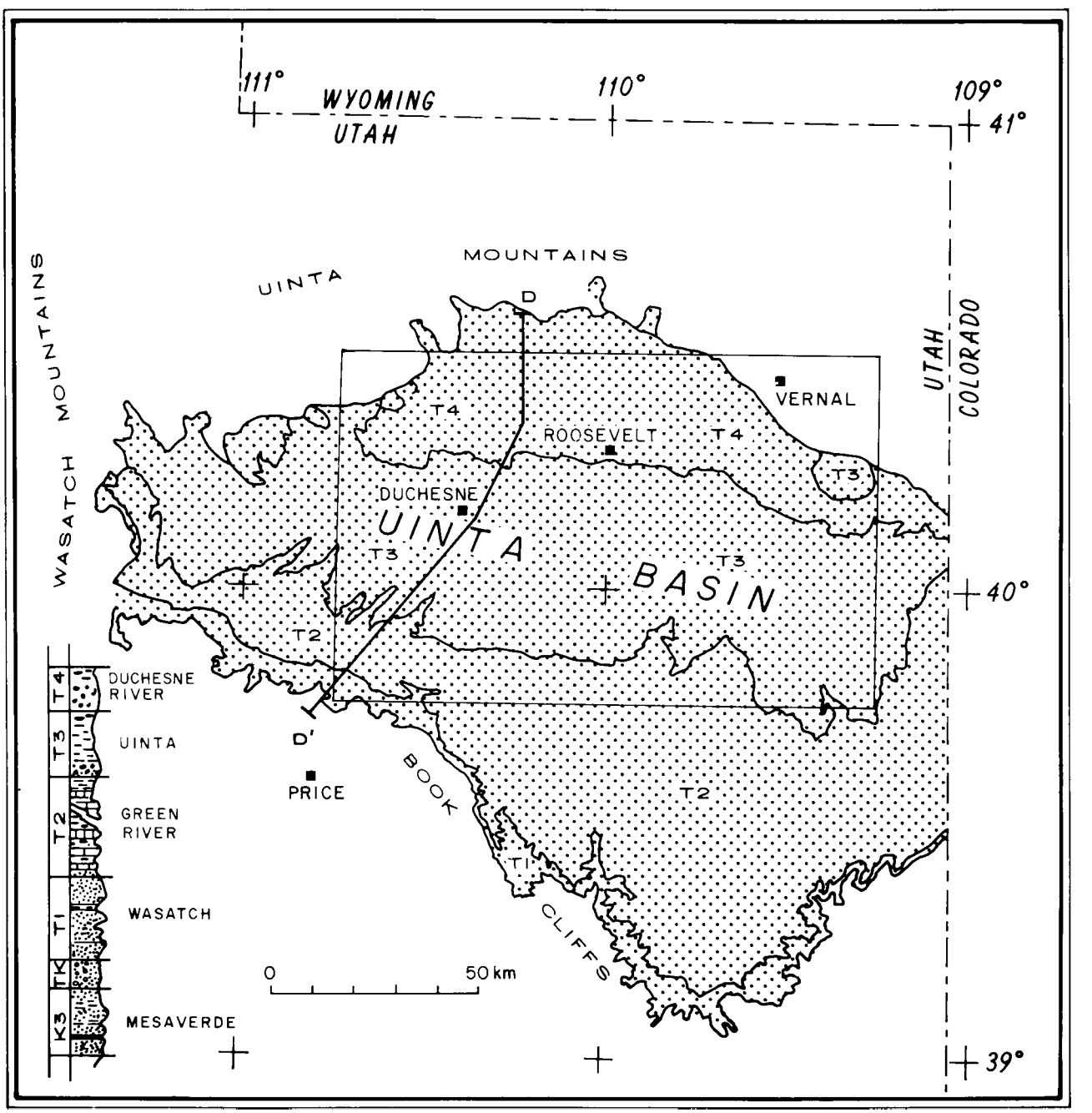

FIG. 2. Location map for the Uinta Basin, northeastern Utah. Shaded area indicates Tertiary outcrops. Rectangle is study area for reference in Figures 7, 10, and 11. Lower left inset shows conventional stratigraphic column for Upper Cretaceous (K3), Cretaceous-Tertiary (TK), and Tertiary (T1 through T4) formations shown on the map and discussed in the text.

from about 13.7 km in the eastern part of the basin to about 19.2 km in the western part. Approximately 4.5 km of the stratigraphic sequence is Tertiary in age.

The Tertiary system of the Uinta Basin (Figure 3) (Bradley, 1931; Picard, 1957; Preston, 1957; Murany, 1964; Untermann and Untermann, 1964; Ryder et al, 1976) began with withdrawal of the Cretaceous sea related to uplift on the west and north. As a result, marine claystone and siltstone grades laterally and is interbedded with nonmarine sandstone, shale, siltstone, and coal seams of channel floodplain and lagoonal character. The final phase of Cretaceous deposition and the first phase of Tertiary deposition are represented by continental facies of clastic rocks. The Cretaceous-Tertiary boundary is difficult to place with certainty.

Coalescing of small freshwater lakes in the western part of the basin brought an end to widespread fluvial deposition (Wasatch formation and equivalents—North Horn, lacustrine Flagstaff, Colton) of the early Tertiary. Two major periods of lacustrine deposition then followed, and the Flagstaff limestone and Green River formation were deposited. Of these, the Green River formation, deposited in Lake Uinta, is more extensive in the Uinta Basin. The complex interfingering of fluvial and deltaic beds with those of lacustrine origin indicates that Lake Uinta, which was probably stable for long periods and is estimated (Picard and High, 1972) to have existed for about 13 million years, underwent many fluctuations as it transgressed across its broad flood plain. In later stages, the lake increased in salinity and gave way to an interfingering of fluvial and lacustrine sediment (Uinta formation of late Eocene age) as it withdrew to the west-central part of the basin.

Deposition of the fluvial Duchesne River formation (probably latest Eocene but perhaps Oligocene for the uppermost member) followed as downwarping ceased and the basin filled with fluvial beds as streams were again the major agents of deposition (Andersen and Picard, 1974).

Along the northern edge of the basin, against the south flank of the Uinta Mountains, Tertiary formations progressively overlap the upturned and eroded edges of pre-Tertiary formations. There, maximum warping has produced the Uinta Basin syncline where dips vary from 10 to 35 degrees on the north limb, but flatten to 2 to 4 degrees on the south limb (Figure 3).

Structure of the basin is relatively simple. Formation contacts form simple concave upward surfaces that can be described by two-dimensional low-order polynomial surfaces with no more than a hundred meters or so misfit to identified contacts across the basin. The interfingering of deltaic, fluvial, and lacustrine deposits from several source areas, in contrast, has resulted in complex lateral facies changes within Tertiary formations with consequent complications for deriving thermal conductivity profiles.

ANALYSIS

Data

The basic data set consists of information from approximately 2000 wells in the area defined by latitudes 39.77°N to 40.50°N and longitudes 109.00°W to 110.75°W which were made available from the WEXPRO Petroleum Information file. The quality and completeness of data in the master file is variable. We required, for instance, knowledge of formation thicknesses for our thermal resistance calculation, and found in the entire data set only 1200 wells with the top of the Green River formation entered, 1000 with the top of the Wasatch formation, and 70 with the top of the Uinta formation. In contrast, surface elevations are included for all wells. Bottomhole temperatures are available for most of the wells, but the correction for drilling disturbances requires multiple BHT measurements at successive times in order to extrapolate to an equilibrium temperature. This requirement eliminates most of the wells and limits the data set of wells with correctable temperatures to approximately 5 percent of all wells in the

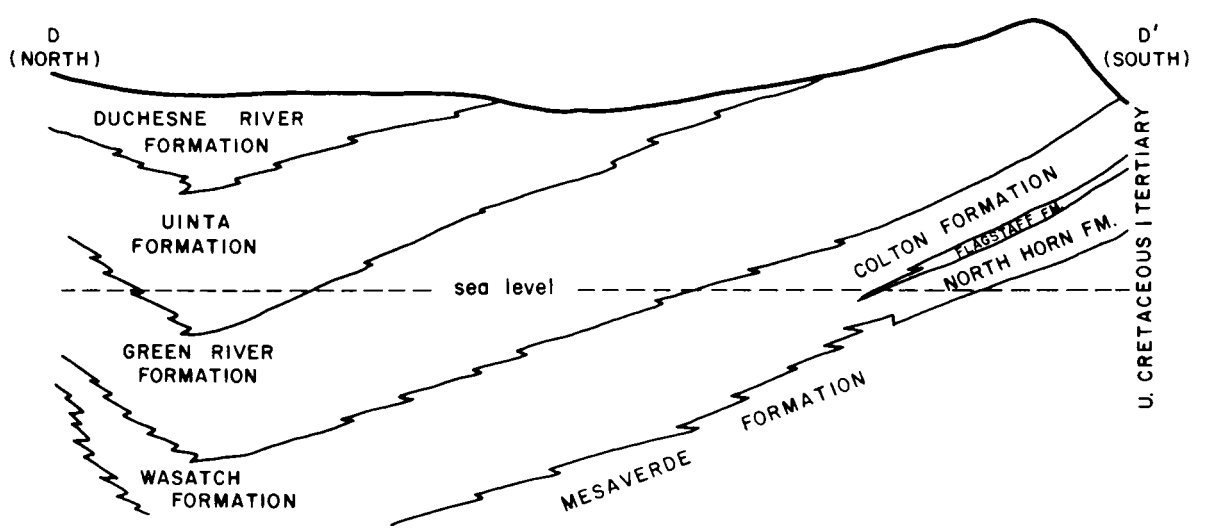

FIG. 3. Schematic north-south cross-section through the Uinta Basin. Section follows profile DD' of Figure 2. Length of the profile is 120 km. Maximum thickness of the Tertiary sequence (Duchesne River through Wasatch Formations) shown is about 4300 m.

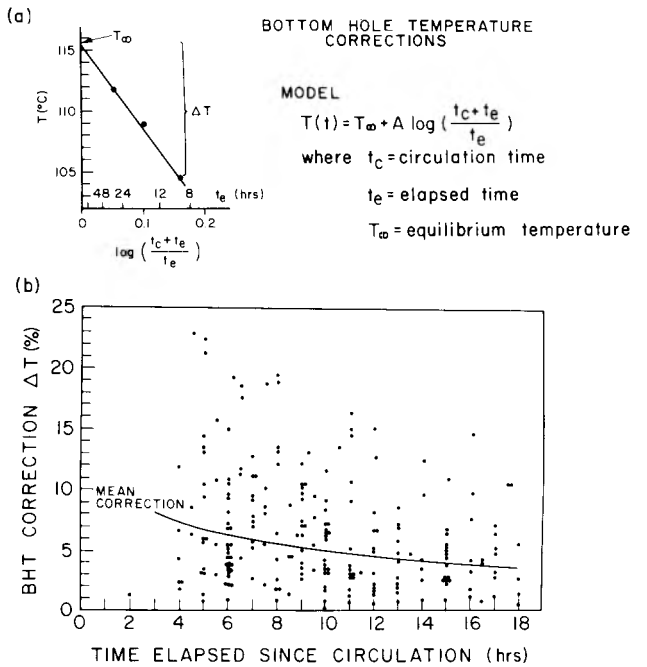

FIG. 4. (a) An example of a BHT correction. Multiple log readings 9, 16, and 32 hours after circulation ceased are used to extrapolate to the equilibrium temperature T_∞. (b) Magnitude of bottom-hole correction, expressed as a percentage of the observed value in °C, as a function of elapsed time after circulation, for 97 wells with multiple BHT values recorded.

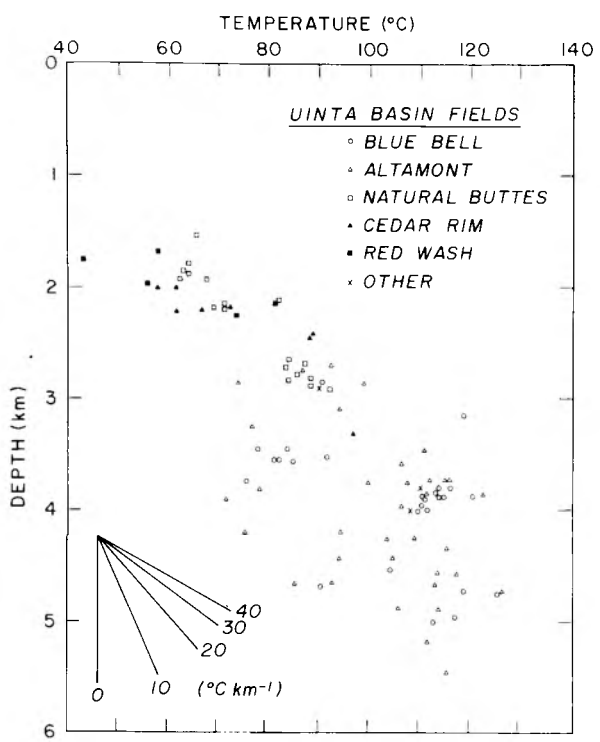

FIG. 5. Corrected bottom-hole temperatures versus depth for 97 wells distributed over the Uinta Basin. Wells are coded with respect to the producing fields.

basin. Few wells drilled prior to 1960 meet this requirement. From the more recent wells with multiple measurements we eliminated those that had identical temperatures recorded for several log runs, believing that a temperature was measured on one log run only and simply recorded on later logs. By carefully searching well logs from the 2000 wells in the Unita Basin, we identified 97 wells for which we could calculate a credible, corrected, bottom-hole temperature.

Five wells were sampled for thermal conductivity measurements. These wells were chosen from those available at the core library of the Utah Geological and Mineral Survey on the basis of having continuous samples from near the surface to below the Wasatch formation. The shallow Cottonwood Springs well was chosen to obtain additional samples from the Duchesne River formation. The wells were also chosen to be as close as possible to areas with concentrations of BHT data while also sampling different areas of the basin. Hindsight suggests that we undersampled the basin in a lateral sense.

Temperatures

Detailed temperature data were taken from well logs. Because of several factors, primarily, fluid circulation before logging, bottom-hole temperatures from well logs are lower than static formation temperatures. The Horner technique (Dowdle and Cobb, 1975; for discussion see Table 1, Lachenbruch and Brewer, 1959) is a method commonly used to correct these temperatures. The technique involves plotting the bottom-hole temperature in a given well versus time according to the equation

$$T_B(t) = T_{B,\infty} + A \log\left(\frac{t_c + t_e}{t_e}\right), \tag{3}$$

where t_c is the circulation time, t_e is the time elapsed since circulation, and $T_B(t)$ is the time-dependent BHT. By plotting $\log [(t_c + t_e)/t_e]$ against T, one can estimate $T_{B,\infty}$, the true formation temperature, as the ordinate intercept as shown in Figure 4a. When the circulation time that corresponds to a BHT measurement was unknown, a standard circulation time of 4 hours was used.

Ninety-seven wells were found in which the bottom-hole temperature was recorded accurately more than once, thus allowing for a determination of the constant A and application of the Horner technique. The determination of A and $T_{B,\infty}$ was done by linear regression. The majority of the wells are located in the Altamont-Bluebell-Cedar Rim trend in Duchesne County north and northeast of Duchesne. Most of the others are in the Natural Buttes field of Uinta County flanking the White River. Bottom-hole temperatures were measured at depths ranging from 1500 m in Natural Buttes to 5500 m in Altamont-Bluebell. These depths correspond to the lower Green River and upper Wasatch formations. Corrected temperatures from the wells are plotted versus depth in Figure 5. The wide scatter indicates that the geothermal gradient is nonuniform throughout the basin. The mean geothermal gradient for the basin from these data is 25°C km^{-1}.

Since the vast majority (about 95 percent) of wells in the Uinta Basin do not have sufficient data for correction by the Horner technique, it is appropriate to investigate the likely error involved if raw uncorrected temperature data were to be used and also the possibility of reducing this error by applying some empirical corrections to the raw temperature data. For this purpose we performed a test using the 97 wells with multi-

ple temperature measurements for which we were able to compute an estimate for the equilibrium temperature (i.e., $T_{B,\infty}$). The difference between this computed equilibrium temperature ($T_{B,\infty}$) and any measured temperature (T_B) can be regarded as the correction necessary for that measurement. The percentage corrections for all measurements are plotted in Figure 4b against time elapsed since circulation when the measurement was made. Three observations can be made. First, all the corrections are positive for this data set, indicating that drilling at these depths produced a cooling effect. Second, errors up to 25 percent may exist in individual measurements made soon after drilling; the correction limit decreases to about 12 percent after 18 hours of elapsed time. Third, a typical correction for this data set (shown as a solid line in Figure 4b) has the form $T_{B,\infty} = T_B(1.11 - 0.026 \ln t_e)$ which amounts to a 7 percent correction for an elapsed time of 4 hours, falling to 3 percent after 20 hours, although there is considerable scatter in the data. The magnitude of this correction agrees with corrections proposed by others. Schoeppel and Gilarranz (1966) suggested that maximum logged temperatures of deep wells are within 5 percent of true static formation temperatures. Carvalho and Vacquier (1977) stated that for elapsed times greater than 10–12 hours the BHTs are accurate to within 8 percent of the true static formation temperatures. For the test data shown in Figure 4b, 80 percent of the data points fall within ± 5 percent of the mean correction based on elapsed time only. This is a tolerable uncertainty for treating new uncorrected temperature data as long as little significance is placed on isolated temperature anomalies which may simply be part of the population outside these limits. Other empirical correction factors based on depth alone (AAPG, 1972) or by depth, circulation time, measurement time, and regional geothermal gradient (Scott, 1982) may provide further improvements in reducing uncertainties in BHT data. Alternative approaches and refinements recently suggested by Middleton (1979, 1982), Leblanc et al (1981), and Lee (1982) for thermal stabilization of a drill hole can also be used where knowledge of thermal properties of drilling mud and wall rock are known. However, in this study we defer further discussion of using uncorrected BHT data and restrict our analysis to the 97 wells where equilibrium temperatures were calculated.

Thermal conductivity

All thermal conductivity values were determined using the modified divided bar designed by Blackwell (Roy et al, 1968) and similar in operation to that described by Sass et al (1971b). The bar was calibrated with standards of fused silica and crystalline quartz using temperature-dependent conductivity given by Ratcliffe (1959) and a procedure given by Chapman (1976) which accounts for lateral heat losses and sample contact resistance. Reproducibility of thermal conductivity determination is typically better than 2 percent and interlaboratory agreement between measurements on identical samples is better than 5 percent (Chapman, 1976). For drill cuttings we used the cell technique of Sass et al (1971a).

Five wells in the Uinta Basin were sampled for detailed thermal conductivity measurements: Rock Creek, Fisher, Cottonwood Springs, Red Wash, and South Ouray. We initially sampled the wells at 30 m intervals, which gave between 10 and 20 samples per formation per well. The sample interval was decreased to 15 m when erratic behavior in the conductivity profile was observed. The increased sample density corresponded to a plan of characterizing basin thermal conductivity in terms of members of formations rather than by entire formations. Subsequent analysis indicates that for the Uinta Basin this is misguided sampling. It would have been preferable to sample a greater number of wells having a broader geographic distribution with fewer samples per formation.

Thermal conductivity results for the five wells are shown in Figure 6. In each figure we have plotted the individual results for all samples measured, together with a histogram representing each formation. Numbers of samples, conductivity, and standard deviation are given in Table 2.

The variety in the thermal conductivity results, both in the formation means between wells and in the distribution of values in a single well, reflects primarily the complex depositional history of the Tertiary Uinta Basin formations. For the South Ouray well (Figure 6) conductivities of all formations are well constrained, as indicated by tight distributions and standard deviations between 0.3 and 0.5 $Wm^{-1}K^{-1}$. In other wells certain formation conductivities are poorly constrained, as for example in the Duchesne River formation in the Fisher well

Table 2. Thermal conductivity results for the Uinta Basin.

	Formations														
	Duchesne River			Uinta			Green River			Wasatch			Mesaverde		
Well	N	k	s.d.	N	k	s.d.	N	k	s.d.	N	k	s.d.	N	k	s.d.
Rock Creek				41	4.37	0.94	135	3.13	0.80						
Fisher	28	4.80	1.65	77	2.78	0.59	106	3.15	0.86	75	2.57	0.30			
Cottonwood Springs	23	4.81	0.35	17	4.37	0.78									
Red Wash				15	2.44	0.41	58	3.70	1.55	37	2.89	0.40	32	2.80	0.79
South Ouray				49	2.12	0.41	53	2.22	0.48	59	2.29	0.38	47	2.79	0.31
(Mean)	51	4.80		199	3.22		352	3.05		171	2.58		79	2.80	

Notes: N is number of samples; k is mean thermal conductivity in $Wm^{-1}K^{-1}$; s.d. is standard deviation in $Wm^{-1}K^{-1}$. Measurements were made on drill chip samples in the laboratory at 20°C and represent the solid matrix conductivity at that temperature. Actual formation thermal conductivity must be corrected for fluid, porosity, and temperature effects as described in text and Table 1.

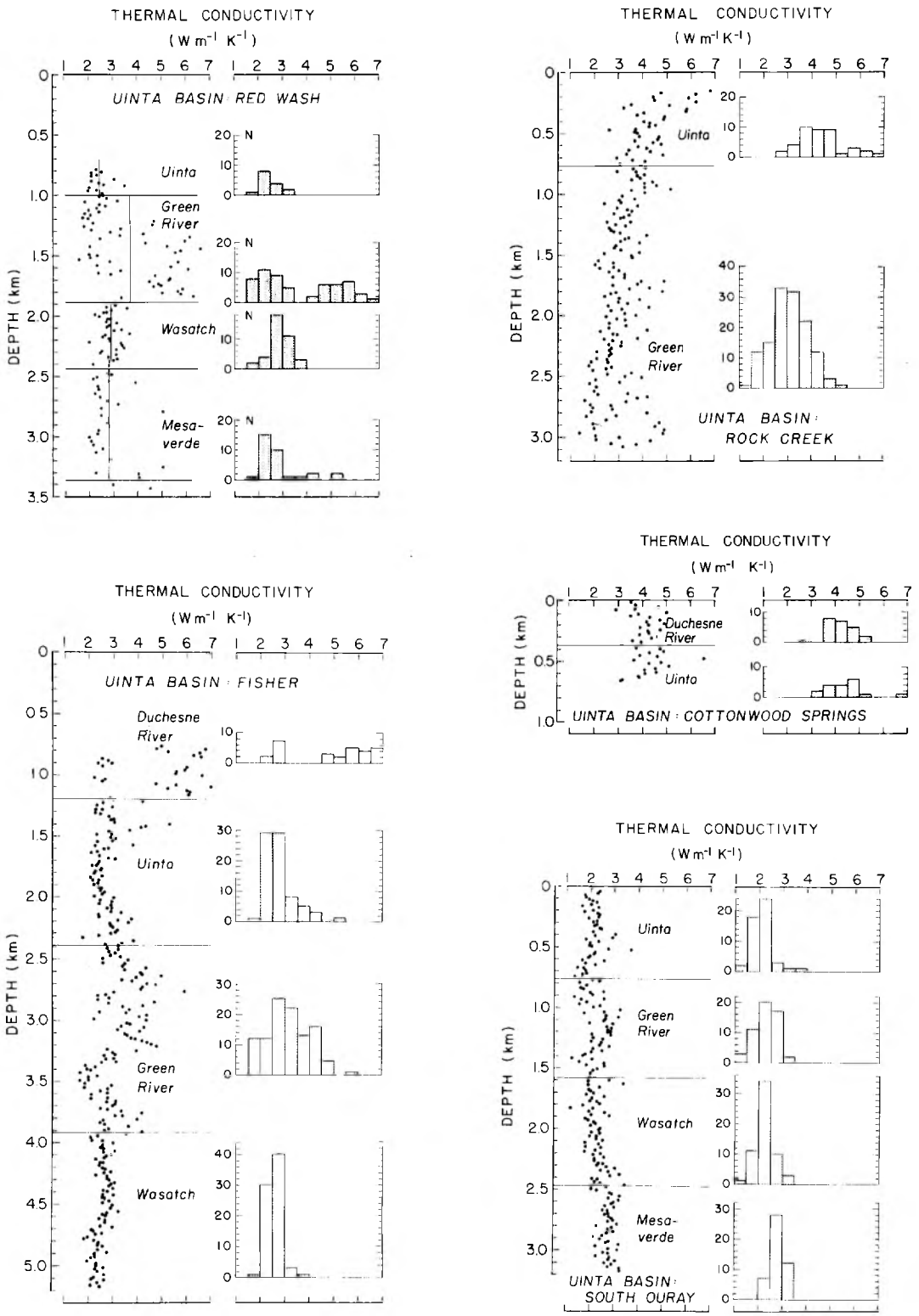

FIG. 6. Thermal conductivity results for five wells in the Uinta Basin. Well locations are shown in Figures 7, 10, and 11. Left side of the figures shows results for individual samples; right side shows histograms of results for each formation in each well. Measurements were made on drill chip samples in the laboratory at 20°C and represent the solid matrix conductivity at that temperature. Actual formation thermal conductivity must be corrected for fluid, porosity, and temperature effects as described in the text and Table 1.

(Figure 6) and in the Green River formation in the Red Wash well (Figure 6) where standard deviations are 1.5 to 1.7 $Wm^{-1}K^{-1}$. In the latter cases the distribution is bimodal because of interbedded sandstone-claystone intervals where the coarser components are characterized by conductivities of 5–7 $Wm^{-1}K^{-1}$, in contrast to claystone-rich beds having conductivities of 1.5–3 $Wm^{-1}K^{-1}$.

Average thermal conductivities given in Table 2 are consistent with values reported in previous studies. Reiter et al (1979) reported a mean conductivity for the Evacuation Creek and upper Parachute Creek members of the Green River formation in the Red Wash field of 2.32 (s.d. 0.25) $Wm^{-1}K^{-1}$. For the same interval in the Red Wash well, the mean for our measurements is 2.50 (s.d. 0.95) $Wm^{-1}K^{-1}$. A second comparison can be made in the South Ouray field. The mean value for the Uinta formation of 2.14 (s.d. 0.45) $Wm^{-1}K^{-1}$ determined in well W-EX-1 by Sass and Munroe (1974) agrees closely with our value of 2.12 (s.d. 0.41) $Wm^{-1}K^{-1}$ (see Table 2).

A less welcome feature of the thermal conductivity results is the variation from well to well in any given formation. The Uinta formation, for example, has a conductivity greater than 4 $Wm^{-1}K^{-1}$ in the Rock Creek and Cottonwood Springs wells, 2.78 $Wm^{-1}K^{-1}$ in the Fisher well, 2.44 $Wm^{-1}K^{-1}$ at Red Wash, and only 2.12 $Wm^{-1}K^{-1}$ at South Ouray. The Green River formation exhibits similar variations. While such patterns are consistent with the facies changes—the high Green River formation conductivity at Red Wash, for example, coincides with an extensive depositional tongue characterized by high sandstone content—the patterns complicate the processing of data on a basin scale.

The common assumption of constant thermal conductivity within a formation, which is reliable for the Mesozoic sedimentary rocks of the central Colorado Plateau on the south (Bodell and Chapman, 1982), is clearly in error in the Uinta Basin. As a consequence, we have developed maps of lateral thermal conductivity variations within the basin.

For each formation we assembled facies maps, cross-sections, available stratigraphic columns, and estimates of sand/clay ratios. By combining this information with the correlation between thermal conductivity and rock type available from our measurements on the 852 samples, we developed the thermal conductivity maps shown in Figure 7 for the Uinta, Green River, Wasatch, and Mesaverde formations. We had insufficient information to discern any systematic variations within the Duchesne River formation other than the decrease in conglomerate clast size eastward across the basin and the decrease in grain size from north to south. The pattern in each formation strongly reflects depositional environment; open lacustrine rocks, for example, generally contain a higher clay fraction and thus a lower conductivity. Although differences of a much

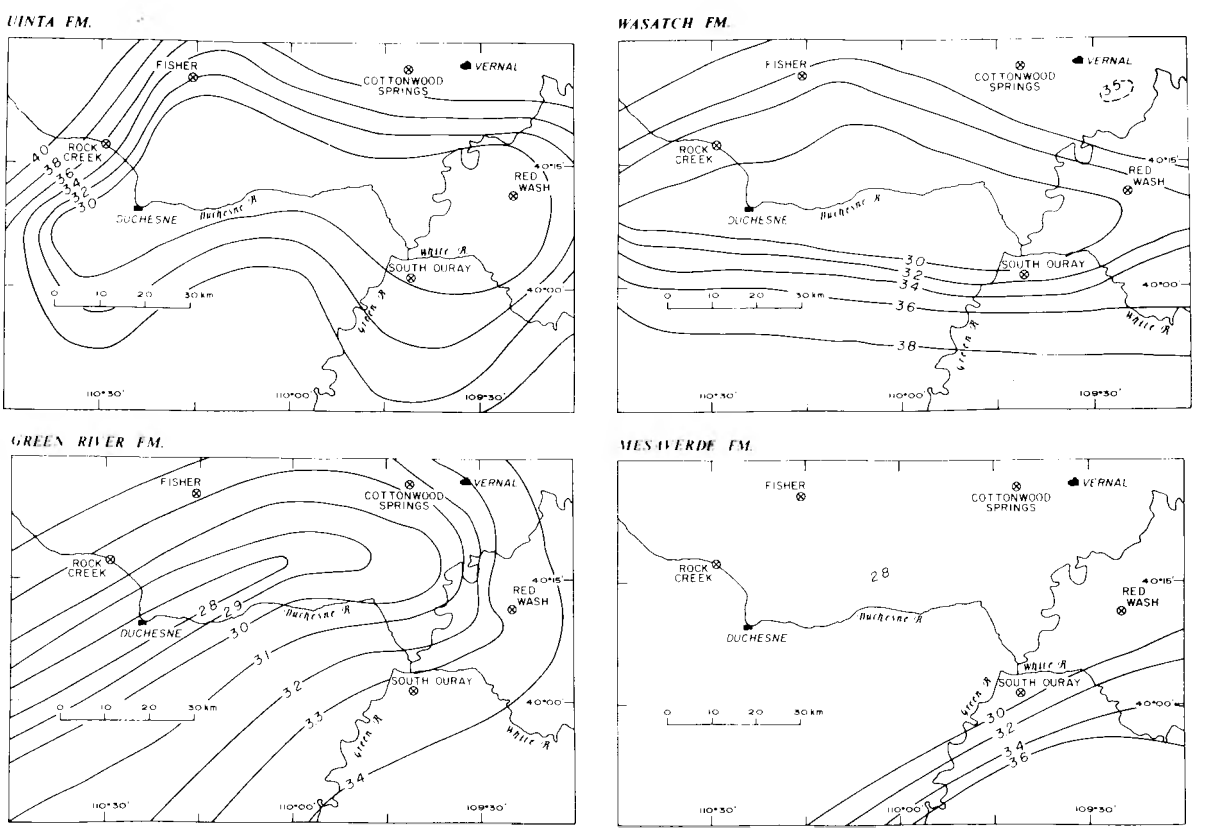

FIG. 7. Thermal conductivity maps of the Uinta, Green River, Wasatch, and Mesaverde formations in the Uinta Basin. Contours represent estimates of the solid component thermal conductivity at 20°C (units $Wm^{-1}K^{-1}$) and are controlled primarily by facies changes. Actual formation conductivity must be corrected for fluid, porosity, and temperature effects.

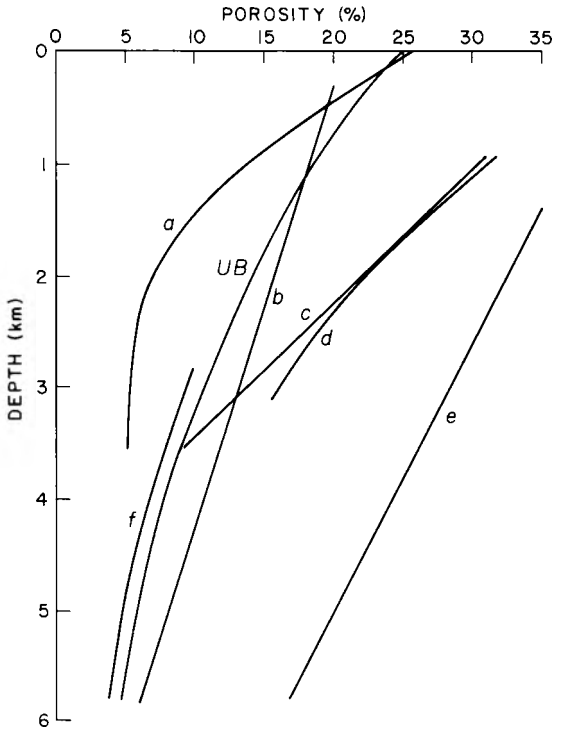

FIG. 8. Porosity depth functions for some typical rock types: (a) Jurassic-Cretaceous shale (Caucasus), (b) Pennsylvanian-Permian sandstone (Texas Okalahoma), (c) Jurassic-Cretaceous sandstone (Caucasus), (d) Jurassic-Cretaceous quartz sandstone, (e) Quaternary sand (Louisiana), (f) Carboniferous silty sandstone. Modified after Jonas and McBride (1977). UB indicates function adopted for the Uinta Basin.

greater magnitude may exist locally, typical conductivity changes across a formation on these smoothed maps are 30 percent. The northwest high-conductivity trend persists through the Uinta and Wasatch formations and may partly explain the lower thermal gradients observed in that part of the basin. For computational purposes, the variations shown in Figure 7 were all expressed in terms of low-order polynomial surfaces by least-squares fitting.

So far the discussion of thermal conductivity values has been based on laboratory measurements of the solid component k_s at room temperature, nominally 20°C. Several corrections must be applied to adjust for in-situ thermal conductivity of porous rocks at elevated temperatures.

For rocks with a porosity ϕ, the water-saturated rock conductivity k_r, appropriate for in-situ conditions, may be calculated as the geometric mean from the pure phase conductivities, weighted according to their fractional volumes

$$k_r = k_w^{\phi} k_s^{(1-\phi)}, \tag{4}$$

where k_w is the conductivity of water. [See Robertson and Peck (1974) for a discussion of this and other possible models for porous rocks and further references.] For a conductivity range of 1.5 to 3.5 $Wm^{-1}K^{-1}$, for example, a 10 percent porosity adjusts the measured conductivity by 9–16 percent and a 20 percent porosity, by 17–30 percent. It was impossible to measure porosities for individual samples, and porosities from well logs are useful only as general indicators. We therefore chose a generalized porosity-depth function to characterize the basin. Figure 8 shows a variety of porosity-depth functions varying from linearly decreasing curves suitable for well-sorted sandstone to exponentially decreasing curves more appropriate for silty and shaly rocks. The distribution chosen for the Uinta Basin based on reports for porosity at specific horizons and concensus of personal communications is

$$\phi = 0.25 \exp(-z/3.0) \tag{5}$$

where z is depth in kilometers. This relation yields a porosity of 25 percent at the surface and 5 percent at 4.8 km depth.

Temperature dependences for water conductivity k_w, assuming that the pores are filled with water, and matrix conductivity k_s are also needed for the conductivity correction. Water has a conductivity of 0.56 $Wm^{-1}K^{-1}$ at 0°C, but it increases to 0.68 $Wm^{-1}K^{-1}$ at 100°C. We have approximated temperature-conductivity data for water given by Kappelmeyer and Haenel (1974) by the following functions:

$$k_w = 0.56 + 0.003T^{0.827}; \qquad 0 \le T \le 63°C \tag{6}$$

$$k_w = 0.481 + 0.942 \ln T; \qquad T > 63°C. \tag{7}$$

These equations were then used to adjust k_w for in-situ conditions in the basin. We have further assumed that the solid matrix conductivity k_s is proportional to the reciprocal of the absolute temperature. Thus

$$k_s = k_{20}[293/(T + 273)], \tag{8}$$

where k_{20} is conductivity determined in the laboratory at 20°C. This correction is significant. For a sample with measured conductivity (20°C) of 3.0 $Wm^{-1}K^{-1}$ the in-situ matrix conductivity varies between 3.1 at the surface (10°C) and 2.2 (135°C) at 5 km depth. No attempt is made to make anisotropy corrections because of the complexity of the problem, considering only drill chips were available for measurement and the relatively small effect it is believed the corrections would have in this situation. However, possible systematic errors introduced by neglecting anisotropy and by making chip measurements on claystones which may have undergone irreversible changes upon drying should not be ignored in the interpretation of results. Blackwell et al (1981) and Sass and Galanis (1983) gave examples of the problem of determining thermal conductivity of shales.

Surface heat flow

This section describes procedures for processing large data sets of BHTs to obtain heat flow patterns and subsurface temperature maps. If, for each well, a corrected BHT is available, and if the rock types are known and can be converted into a thermal conductivity profile, the computation of heat flow is relatively simple. In reality the data set is incomplete and approximate techniques must be adopted.

We approximate in some instances the positions of formation contacts by fourth-order polynomial surfaces. The surfaces were generated from pertinent well information; the top of the Uinta formation was available in 70 well records and the Green River and Wasatch formations in about 1000 records each. The choice of fourth-order polynomials to represent the formations was made on the basis of a plot of rms residual (difference between recorded formation position and calculated position

using the polynomial surface) versus polynomial order. Figure 9 shows that formation contacts are adequately expressed as fourth-order surfaces (second order for Wasatch and Green River) and that little benefit is gained by adding higher orders.

One filtering process required for the Uinta Basin concerned raw data where formation tops identified on well logs departed from the polynomial surfaces by several hundred meters. In such a case the data points were eliminated and the surface coefficients were recalculated. This process led to a reduction of 5 percent in the Wasatch formation records, 10 percent in the Green River formation records, and 10 percent in the Uinta formation records. The discrepancy lies partly in the difficulty of identifying formation boundaries, but also in systematic differences between the stratigraphic conventions adopted by different companies. The average rms misfit for each formation after filtering the data is: Uinta formation, top 81 m; Green River formation, top 70 m; and Wasatch formation, top 70 m.

From these polynomial surfaces, depths to formations were obtained for wells in which any formation top was missing, and formation thickness was calculated for use in the thermal resistance calculation. A subroutine was developed to compute porosity-corrected thermal conductivity for each formation at any location. This subroutine computes the average conductivity of water k_w as a function of temperature, the conductivity of the solid component k_s as function of temperature, the average porosity, and the porosity-corrected thermal conductivity for each formation according to the relations described previously. Because the formations are at different depths in different parts of the basin, the porosity and temperature corrections cause the thermal conductivity of each formation to vary laterally in patterns somewhat different from those governed by facies changes shown in Figure 7. Once the conductivities were calculated, all the information was available for the computation of surface heat flow from the thermal resistance equation.

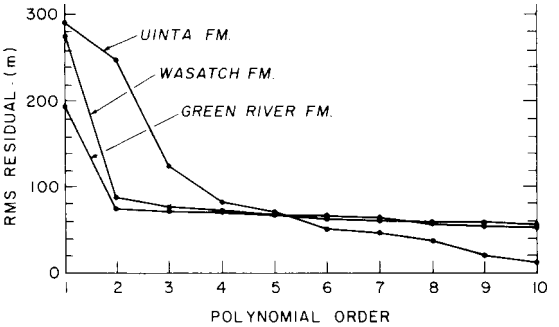

FIG. 9. Root mean square (rms) residuals between position of formation top recorded on well log and position computed from the polynomial surface approximation.

Surface heat flow in the Uinta Basin is shown in Figure 10. After rejecting three anomalous values using the Chauvenet rejection criteria (Beers, 1957, p. 23), the mean heat flow for the 94 wells is 57 mWm^{-2} with a standard deviation of 11 mWm^{-2}. Heat flow varies from 65 to 40 mWm^{-2} on a profile running north from Duchesne. The area to the southeast bordering the White River exhibits no trend in heat flow and illus-

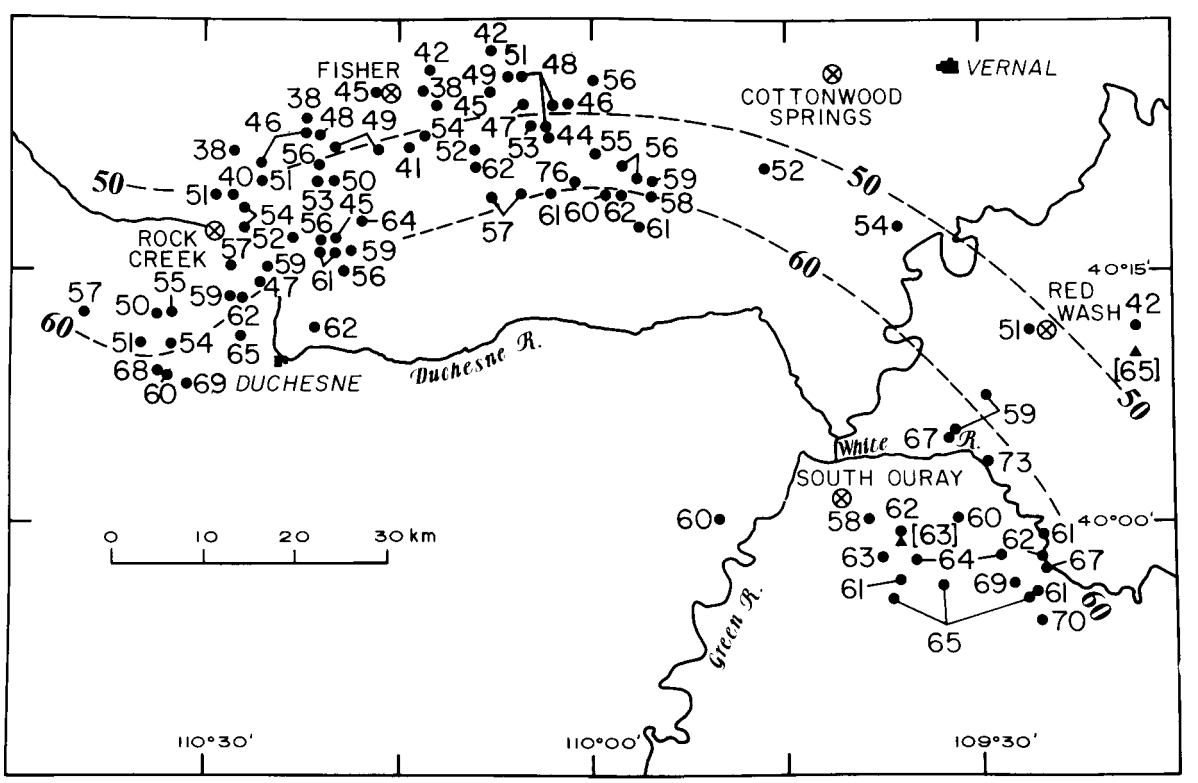

FIG. 10. Surface heat flow for 97 wells (solid dots) in the Uinta Basin computed by the thermal resistance method. Open circles with crosses indicate wells used for thermal conductivity sampling. Triangles give sites of two conventional heat flow determinations with corresponding heat flow values in square brackets.

trates the scatter which can be expected using this method. The range in heat flow computed for 20 wells is 58–73 mWm^{-2}, with a mean and standard deviation of 64 and 4 mWm^{-2}, respectively. We attach no significance to short-range fluctuations of order ± 5 mWm^{-2}, but believe the smooth variations are real.

A test of this treatment of BHT data to produce a heat flow map involves comparing these results with values determined previously in the same area by more conventional heat flow techniques. In this part of the Uinta Basin, only two sites are available for comparison. As shown in Figure 10, the value of 63 mWm^{-2} determined by Sass et al (1971b) at South Ouray over a depth range 61 to 907 m is surrounded by our values of 63, 60, 64, 61, and 63 mWm^{-2}. At the eastern boundary (Figure 10) the value of 65 mWm^{-2} given by Reiter et al (1979) for Red Wash departs considerably from our 42 mWm^{-2} on the north, but is closer to the two nearest values on the west of 51 and 59 mWm^{-2}. The lower value from our method in Red Wash may result from our smoothed conductivity assumption within formations, whereas, in fact, formations undergo rapid facies changes in this region. More likely it is a proper reminder that little significance should be attached to isolated values. A less direct comparison can be made with heat flow determined from conventional heat flow sites to the south of the Uinta Basin. In this sense the Uinta Basin values of 55–65 mWm^{-2} (south of Duschesne and White Rivers, Figure 10) are consistent with the northcentral Colorado plateau values (Table 4 and Figure 8 of Bodell and Chapman, 1982) and in particular with the mean value of 58 mWm^{-2} (31 sites, standard deviation 8 mWm^{-2}) considered representative of the Colorado Plateau interior (Table 5 of Bodell and Chapman, 1982).

Once the surface heat flow pattern is determined, subsurface temperatures at any depth can be calculated by a direct application of the thermal resistance method. An example of temperatures at 1 km depth is shown in Figure 11. The temperature pattern will generally be similar to the heat flow pattern, except where lateral facies variations cause thermal conductivity contrasts. Mean subsurface temperatures in the Uinta Basin are 22 ± 4°C at 500 m depth, 35 ± 7°C at 1000 m, 59 ± 10°C at 2000 m, and 74 ± 12°C at 3000 m.

Error analysis

Throughout the calculation, error propagation was computed using the general formula of Bevington (1969). Since all the errors encountered in formation depths, thermal conductivities, and temperatures were uncorrelated, the covariance terms are all zero. In computations, the average rms errors of the polynomial surfaces were used as the errors of the formation depths whether the depths used were picked formation tops or polynomial computed tops. Accuracy of picked formation tops in the Petroleum Information file is not less than about 50 m (personal communication, J. M. Hummel and C. N. Tripp, 1981). These errors in formation depths result in an

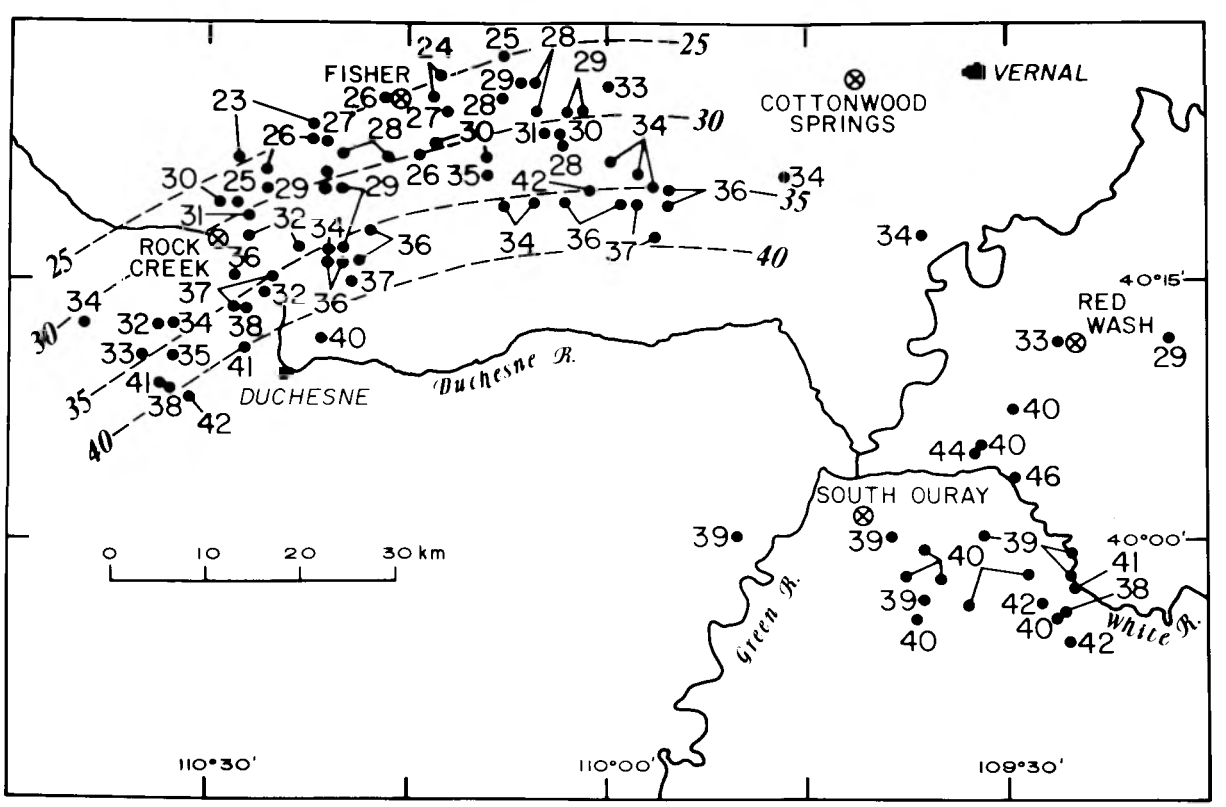

FIG. 11. An example of a subsurface temperature map for the Uinta Basin determined from the heat flow values and application of equation (1) or (2). Temperatures and contours in °C. Such maps are useful for both geothermal utilization and hydrocarbon maturation studies.

average error of 5.6 percent in surface heat flow. An error of 2°C in surface temperature results in an error of about 1 percent in surface heat flow. The standard deviation in formation thermal conductivity, which ranges from 8 to 40 percent, results in a 14 percent error in surface heat flow. The cumulation of these errors results in a total error of about 15 percent in surface heat flow values. Because the errors are uncorrelated, the larger error in thermal conductivity dominates the error propagation. If the error in surface heat flow that is solely the result of conductivity could be reduced from 14 to 10 percent, the cumulative error in surface heat flow would drop to 11 percent. Reducing the error due to conductivity to 5 percent would reduce the cumulation error to 8 percent. These errors may underestimate actual errors if our thermal conductivity measurements on claystones are systematically high, but this effect is difficult to assess.

DISCUSSION

The thermal resistance method described here (see Table 1) and applied to the Uinta Basin is generally applicable to well thermal data in sedimentary basins. The method makes few assumptions of uniformity concerning thermal gradients, thermal conductivity, or homogeneity within the basin. Instead, bottom-hole temperature data are treated individually, together with a best estimate of the vertical thermal conductivity profile at the well site, to produce a local heat flow value. Maps of surface heat flow and subsurface temperatures at arbitrary depths are products of the method.

For the Uinta Basin, we restricted our investigation to 97 wells where BHTs could be corrected for drilling effects. These wells comprise only 5 percent of the wells in the Uinta Basin. The magnitude of temperature corrections for these wells suggests that uncorrected BHTs may differ from equilibrium temperatures by as much as 25 percent, and for the Uinta Basin they are systematically low on the average by 7 to 3 percent depending upon time elapsed after circulation. An empirical mean correction for raw BHT data was developed for the 97 wells in the Uinta Basin such that 80 percent of the computed corrections fall within ± 5 percent of the mean correction. Use of this correction would provide access to a much larger data set (the remaining 95 percent of wells in the Uinta Basin) at an acceptable uncertainty level, provided little significance is attached to isolated temperature anomalies.

The heat flow map (Fig. 10) exhibits local coherency between values and yields a mean value of 57 mWm^{-2}, consistent with heat flow determined by conventional heat flow methods in the Uinta Basin and neighboring areas. Discrepancies of ± 5 mWm^{-2} between adjacent wells are considered to be in the noise.

An interesting feature of the heat flow map, if real, is the pronounced decrease of heat flow within the basin from about 65 to 40 mWm^{-2} as the Uinta Mountains are approached (compare Figures 10 and 2). Although we believe this trend to be real, there remains a possibility that the laboratory measurements of thermal conductivity of claystones and mudstones are systematically in error, or that our BHT correction has a systematic depth-dependent error and that these errors have an effect on our heat flow map. The thermal conductivity explanation is suggested, in part, by the spatial similarity in conductivity maps for the Uinta, Green River, and Wasatch formations in the area north of Duchesne (Figure 7) and the heat flow trend as shown in Figure 10. If the conductivity pattern is interpreted to indicate an increasing clay fraction in a southeast direction toward Duchesne, and if our measured conductivities are systematically high, then heat flow values will be correspondingly overestimated across this trend. However, the same argument should hold true for the South Ouray region where similar gradients are seen in the thermal conductivity maps (Figure 7), but no trend is seen in the surface heat flow (Figure 10). The possibility of a depth-dependent bias was checked by plotting surface heat flow against well depth. Whereas heat flow greater than 60 mWm^{-2} is restricted to wells less than 3900 m depth, heat flow less than 50 mWm^{-2} is found for wells varying in depth from 1800 m to 5500 m. Although there is a general trend toward lower heat flow determined in deeper wells, it is difficult to distinguish between systematic error and a physical process controlled by the basin geometry.

There are at least two heat transfer mechanisms that could produce the lateral heat flow gradient seen in Figure 10. The first mechanism is lateral refraction of heat flow into the very conductive quartzite of Precambrian age which comprises much of the Uinta Mountains on the north. The thermal conductivity contrast between younger Uinta Basin sedimentary rocks and the Precambrian Uinta Mountain Group (quartzarenite, subarkose) may attain a ratio of 1 : 2. Such a contrast would produce a similar 1 : 2 discontinuity in surface heat flow across the contact with basinward values being lower. Observed variations in the heat flow field of 40 to greater than 60 mWm^{-2} are consistent with slightly lesser conductivity constrasts. Theoretical considerations of such a conductive heat transfer problem (see, e.g., Carslaw and Jaeger, 1959, sec. 16.4), however, reveal that for the case of an ellipsoid-shaped basin, heat flow is *uniformly* lowered across the basin. Thus, the lateral surface heat flow gradient within the boundaries of the basin can only be produced by refraction if departures from an elliptical shape are large or if the conductivity field has a more complicated structure than we have assumed.

Another explanation of the heat flow field relies on convective heat transport accompanying the circulation of groundwater. The heat flow pattern in the Uinta Basin (Figure 10) is qualitatively consistent with groundwater recharge at the south flank of the Uinta Mountains, probably localized in the steeply dipping sandstone and limestone beds of late Paleozoic and Mesozoic age, and groundwater discharge or updip water flow south of the east-west basin axis. Although each flow regime needs to be modeled in detail, the general modeling results of Smith and Chapman (1983) on thermal effects of regional-scale groundwater flow systems indicate that the heat flow pattern observed in Figure 10 is consistent with a groundwater flow explanation.

Once the surface heat flow field has been established, subsurface temperatures can be readily calculated for any location in the basin. Differences between temperatures computed by the simple gradient method and those computed by the thermal resistance method, for the Uinta Basin on the average, are smaller than we initially expected. There are almost identical porosity corrected thermal conductivities for the Green River and Uinta formations except for thermal conductivities in the fine-grained, carbonate-rich Parachute Creek member of the Green River formation. The Duchesne River and Wasatch formations have significantly different conductivites, but the Duchesne River formation is absent over two-thirds of the study area and is thin compared with the depths of the BHTs where the Duchesne River formation is present. A better test of

this method would be provided by a basin where sharp contrasts exist in the thermal conductivity of different units.

Subsurface temperature maps for the Uinta Basin show similar spatial variations to the surface heat flow map. Such lateral variations may be overlooked unless heat flow values are computed for individual wells and the heat flow field is mapped. The lateral temperature differences predicted for greater depths within the Uinta Basin have important implications for regional differences in hydrocarbon maturation within the basin.

ACKNOWLEDGMENTS

We thank G. W. Hohmann and Diane I. Doser for critically reading the manuscript and offering suggestions for its improvement. J. M. Hummel, Chief Geologist, and C. N. Tripp of WEXPRO gave assistance and advice. We appreciate the generous access to WEXPRO information in the Uinta Basin. M. A. Mabey and W. Pe assisted with thermal conductivity measurements. S. D. Willett assisted with computations. Financial support was provided by DOE/DGE contract no. DEAC0780ID12079.

REFERENCES

American Association of Petroleum Geologists (AAPG), 1976, Basic data file from AAPG Geothermal Survey of North America: Univ. of Oklahoma, Norman.

Andersen, D. W., and Picard, M. D., 1974, Evolution of synorogenic clastic deposits in the intermontane Uinta Basin of Utah, *in* Tectonics and sedimentation: W. R. Dickinson, Ed., Soc. Econ. Paleont. Min., Special Publ. 22, p. 165–189.

Beers, Y., 1957, Introduction to the theory of error: Reading Mass., Addison-Wesley Publ. Co. 66 p.

Bevington, P. R., 1969, Data reduction and error analysis for the physical sciences: New York, McGraw Hill Book Co., Inc. 336 p.

Blackwell, D. D., Steele, J. L., and Steeples, D. W., 1981, Heat flow determinations in Kansas and their implications for midcontinent heat flow patterns (abstract): EOS Trans. Am. Geophys. Union, v. 62, p. 392.

Bodell, J. M., and Chapman, D. S., 1982, Heat flow in the north-central Colorado Plateau: J. Geophys. Res., v. 87, p. 2869–2884.

Bradley, W. H., 1931, Origin and microfossils of the oil shale of the Green River Formation of Colorado and Utah: U.S.G.S. Prof. Paper 168, 58 p.

Bruhn, R. L., Picard, M. D., and Beck, S. L., 1983, Mesozoic and early Tertiary structure and sedimentology of the central Wasatch Mountains, Uinta Mountains and Uinta Basin: Utah Geological and Min. Survey, in press.

Bullard, E. C., 1939, Heat flow in South Africa: Proc. Roy. Soc. London, Ser. A, v. 173, p. 474–502.

Carslaw, H. S., and Jaeger, J. C., 1959, Conduction of heat in solids, 2nd ed.: New York, Oxford Univ. Press, 510 p.

Carvalho, H. da S., and Vacquier, V., 1977, Method for determining terrestrial heat flow in oil fields: Geophysics, v. 42, p. 584–593.

Carvalho, H. da S., Purwoko, S., Thamrin, M., and Vacquier, V., 1980, Terrestrial heat flow in the Tertiary basin of central Sumatra: Tectonophys., v. 69, p. 163–188.

Chapman, D. S., 1976, Heat flow and heat production in Zambia: Ph.D. Thesis, Univ. of Michigan, Ann Arbor, 94 p.

Chaturvedi, L., and Lory, J. K., 1980, A preliminary evaluation of geothermal potential of San Juan Basin, New Mexico, using bottom hole temperatures from oil and gas wells: Geotherm. Res. Council, Trans., v. 4, p. 21–24.

Dowdle, W. L., and Cobb, W. M., 1975, Static formation temperature from well logs—an empirical method: J. Petr. Tech., p. 1326–1330.

Evans, T. R., and Coleman, N. C., 1974, North Sea geothermal gradients: Nature, v. 247, p. 28–30.

Evans, T. R., and Tammemagi, H. Y., 1974, Heat flow and heat production in northeast Africa: Earth Plan. Sci. Lett., v. 23, p. 349–356.

Goss, R. D., 1974, Empirical relationships between thermal conductivity and other physical parameters in rocks: Ph.D. Thesis, Univ. of California, Riverside, 216 p.

Hodge, D. S., Hilfiker, K., De Rito, R., Maxwell, J., Morgan, P., and Swanberg, C., 1980, Relationship of heat flow and temperature gradients to basement lithology, N.Y.: EOS Trans. Am. Geophys. Union, v. 61, p. 363.

Jonas, E. C., and McBride, E. F., 1977, Diagenesis of sandstone and shale: Application to exploration for hydrocarbons: Univ. of Texas at Austin, Continuing. Ed. Program, Publ. 1, 165 p.

Kappelmeyer, O., and Haenel, R., 1974, Geothermics with special reference to application: Geoexploration Monograph Ser. 1, No. 4, Berlin-Stuttgart, Gebr. Borntraeger, 238 p.

Kehle, R. B., 1972, Geothermal survey of North America, 1971, Annual Progress Report: Am. Assoc. Petr. Geol., 31 p.

Klemme, H. D., 1975, Geothermal gradients, heat flow and hydrocarbon recovery, *in* Petroleum and global tectonics: A. G. Fischer and S. Judson, Ed., Princeton, New Jersey, Princeton Univ. Press, p. 251–304.

Lachenbruch, A. H., and Brewer, M. C., 1959, Dissipation of the temperature effect of drilling a well in Arctic Alaska: U.S.G.S. Bull. 1083-C, p. 73–88.

Lam, H. L., Jones, F. W., and Lambert, C., 1982, Geothermal gradients in the Hinton area of west-central Alberta: Can. J. Earth Sci., v. 19, p. 755–766.

Leblanc, Y., Pascoe, L. J., and Jones, F. W., 1981, The temperature stabilization of a borehole: Geophysics, v. 46, p. 1301–1303.

Lee, T. C., 1982, Estimation of formation temperature and thermal property from dissipation of heat generated by drilling: Geophysics, v. 47, p. 1577–1584.

Middleton, M. F., 1979, A model for bottom-hole temperature stabilization: Geophysics, v. 44, p. 1458–1462.

——— 1982, Bottom-hole temperature stabilization with continued circulation of drilling mud: Geophysics, v. 47, p. 1716–1723.

Murany, E. E., 1964, Wasatch formation of the Uinta Basin, *in* Guidebook to the geology and mineral resources of the Uinta Basin: E. F. Sabatka, Ed., Intermountain Assn. of Petroleum Geologists, p. 145–155.

Picard, M. D., 1957, Green River and lower Uinta formations—Subsurface stratigraphic changes in central and eastern Uinta Basin, Utah, *in* Guidebook to the geology of the Uinta Basin: O. G. Seal, Ed., Intermountain Assn. of Petr. Geol., p. 116–130.

Picard, M. D., and High, L. R., Jr., 1972, Criteria for recognizing lacustrine rocks, *in* recognition of ancient sedimentary environments: J. K. Rigby, and W. K. Hamblin, Eds., Soc. of Econ. Palen. and Mineral., Spec. Pub. 16, p. 108–145.

Preston, D. A., 1957, A general discussion of the geologic history of northeastern Utah, *in* Guidebook to the geology of the Uinta Basin: O. G. Seal, Ed., Intermountain Assn. of Petroleum Geologists, p. 21–24.

Ratcliffe, E. H., 1959, Thermal conductivities of fused and crystalline quartz: British J. Appl. Phys., v. 10, p. 22–25.

Reiter, M., and Tovar, J. C., 1982, Estimates of terrestrial heat flow in northern Chihuahua, Mexico, based on petroleum bottom hole temperatures: Geol. Soc. of Am. Bull., v. 93, p. 613–624.

Reiter, M. A., Mansure, A. J., and Shearer, C., 1979, Geothermal characteristics of the Colorado Plateau: Tectonophys., v. 61, p. 183–195.

Robertson, E. C., and Peck, D. L., 1974, Thermal conductivity of vesicular basalt from Hawaii: J. Geophys. Res., v. 79, p. 4875–4888.

Roy, R. F., Decker, E. R., Blackwell, D. D., and Birch, F., 1968, Heat flow in the United States: J. Geophys. Res., v. 73, p. 5207–5221.

Ryder, R. T., Fouch, T. D., and Elison, J. H., 1976, Early Tertiary sedimentation in the western Uinta Basin: Geol. Soc. of Am. Bull., v. 87, p. 496–512.

Sass, J. H. and Galanis, S. P., Jr., 1983, Temperatures, thermal conductivity, and heat flow from a well in Pierre Shale near Hayes, South Dakota: U.S.G.S. open-file Rep. 83–25, 10 p.

Sass, J. H., Lachenbruch, A. H., and Munroe, R. J., 1971a, Thermal conductivity of rocks from measurements on fragments and its application to heat flow determinations: J. Geophys. Res., v. 76, p. 3391–3401.

Sass, J. H., Lachenbruch, A. H., Munroe, R. J., Greene, G. W., and Moses, T. H., Jr., 1971b, Heat flow in the western United States: J. Geophys. Res., v. 76, p. 6376–6413.

Sass, J. H., and Munroe, R. J., 1974, Basic heat-flow data from the United States: U.S.G.S. open-file rep. 74-9, 426 p.

Schoeppel, R. J., and Gilarranz, S., 1966, Use of well log temperatures to evaluate regional geothermal gradients: J. Petr. Tech., v. 18, p. 667–673.

Scott, G. N., 1982, Temperature equilibration in boreholes—A statistical approach: M. S. Thesis, Univ. of Michigan, Ann Arbor, 63 p.

Smith, L., and Chapman, D. S., 1983, On the thermal effects of groundwater flow—1. Regional scale systems: J. Geophys. Res., v. 88, p. 593–608.

Untermann, G. E., and Untermann, B. R., 1964, Geology of Uintah County: Utah Geological and Min. Surv. Bull. 72, 112 p.

Vacquier, V., 1981, Calculation of thermal conductivity from lithologic logs and laboratory measurements on oil well cores, a review: Abstract from Am. Assoc. of Petr. Geol. Research Conf. on the Geothermal Environment of Oil and Gas, Sante Fe, New Mexico.